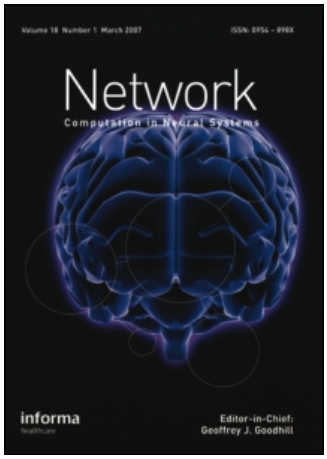

Network: Computation in Neural Systems
Publication details, including instructions for authors and subscription information:
http://www.informaworld.com/smpp/title~content=t713663148

A population approach to cortical dynamics with an application to orientation tuning

A. Omurtag [a]; E. Kaplan [bc]; B. Knight [ac]; L. Sirovich [ac]
[a] Laboratory of Applied Mathematics, Mount Sinai School of Medicine, New York, NY, USA
[b] Department of Ophthalmology, Mount Sinai School of Medicine, New York, NY, USA
[c] The Rockefeller University, New York, NY, USA

Online Publication Date: 01 November 2000

To cite this Article: Omurtag, A., Kaplan, E., Knight, B. and Sirovich, L. (2000) 'A population approach to cortical dynamics with an application to orientation tuning', Network: Computation in Neural Systems, 11:4, 247 — 260

To link to this article: DOI: 10.1088/0954-898X/11/4/301
URL: http://dx.doi.org/10.1088/0954-898X/11/4/301

Network: Comput. Neural Syst. **11** (2000) 247–260. Printed in the UK PII: S0954-898X(00)17406-8

A population approach to cortical dynamics with an application to orientation tuning

A Omurtag†‖, E Kaplan‡§, B Knight†§ and L Sirovich†§

† Laboratory of Applied Mathematics, Mount Sinai School of Medicine, Box 1012, One Gustave L Levy Place, New York, NY 10029, USA

‡ Department of Ophthalmology, Mount Sinai School of Medicine, Box 1012, One Gustave L Levy Place, New York, NY 10029, USA

§ The Rockefeller University, New York, NY 10021, USA

E-mail: ahmet@camelot.mssm.edu

Received 25 April 2000

Abstract. A typical functional region in cortex contains thousands of neurons, therefore direct neuronal simulation of the dynamics of such a region necessarily involves massive computation. A recent efficient alternative formulation is in terms of kinetic equations that describe the collective activity of the whole population of similar neurons. A previous paper has shown that these equations produce results that agree well with detailed direct simulations. Here we illustrate the power of this new technique by applying it to the investigation of the effect of recurrent connections upon the dynamics of orientation tuning in the visual cortex. Our equations express the kinetic counterpart of the hypercolumn model from which Somers *et al* (Somers D, Nelson S and Sur M 1995 *J. Neurosci.* **15** 5448–65) computed steady-state cortical responses to static stimuli by direct simulation. We confirm their static results. Our method presents the opportunity to simulate the data-intensive dynamical experiments of Ringach *et al* (Ringach D, Hawken M and Shapley R 1997 *Nature* **387** 281–4), in which 60 randomly oriented stimuli were presented each second for 15 min, to gather adequate statistics of responses to multiple presentations. Without readjustment of the previously defined parameters, our simulations yield substantial agreement with the experimental results. Our calculations suggest that differences in the experimental dynamical responses of cells in different cortical layers originate from differences in their recurrent connections with other cells. Thus our method of efficient simulation furnishes a variety of information that is not available from experiment alone.

1. Introduction

Although the orientation tuning of neurons in the visual cortex was discovered well over three decades ago (Hubel and Wiesel 1962, 1968), its underlying mechanism remains controversial. While there is a consensus that the early suggestion of a parallel layout of orientation selectivity (Hubel and Wiesel 1968, 1974) should be replaced by a pinwheel arrangement (Bonhoeffer and Grinvald 1991, Blasdel 1992) on the cortex, there is no such accord with respect to the origin of orientation tuning. In simplest terms the issue rests on whether the connectivity pattern from the lateral geniculate nucleus (LGN) suffices to account for orientation tuning, or whether cortical processing of the LGN input is needed as well. The issues and evidence for both views have been the subject of recent reviews (Das 1996, Sompolinsky and Shapley 1997). New support for the role of cortical processing has come from recent innovative experiments (Ringach *et al* 1997), in which the dynamics of orientation tuning was determined by the method of reverse

‖ Corresponding author.

correlation (de Boer and Kuyper 1968, Jones and Palmer 1987). Some additional evidence comes from the recent direct simulation of the cortical steady-state response to static orientation stimuli by Somers *et al* (1995), in which the phenomenon is modelled by cortical feedback acting in conjunction with the LGN input. Another recent model (Adorjan *et al* 1999) is based on anisotropic intracortical excitatory connections, which provide both an initial orientation bias and its subsequent amplification. In the present investigation we consider a dynamical model of early vision, which appends the recently quantified dynamics of retinal ganglion and LGN neurons (Benardete and Kaplan 1999) to the cortical model advanced by Somers and his colleagues. A major difference in approach lies in our use of a *kinetic* description of the neuronal sub-populations that subserve orientation tuning. This approach provides a far more efficient method for simulating the dynamics of the relevant neuronal sub-populations, and enables us also to simulate experiments in which rapid changes of stimuli are presented continually over extended periods of time.

Any attempt to simulate the dynamics of cortical populations of neurons must deal with the immensity of their number, the complexity of their connections and the observed range of dynamic timescales. To face these issues we have developed a *probabilistic* formulation that follows the dynamics in terms of interacting sub-populations of neurons (Knight *et al* 1996, Knight 2000, Omurtag *et al* 2000). In the cited references we derive general kinetic equations for populations of neurons which follow from individual neuronal dynamics without introducing approximations.

Based on the deliberations presented in these papers we have developed a general purpose, flexible numerical code that follows the dynamics of interacting sub-populations of neurons under prescribed conditions. In this paper we use this tool for the exploration of orientation tuning in the primary visual cortex.

When static orientation stimuli are introduced in our kinetic equation simulations we obtain excellent agreement with the direct simulations of Somers *et al* (1995), which underline the suggestion that intra-cortical processing plays an important role in the sharpening of tuning. We have gone on to simulate the experimental paradigm used by Ringach *et al* (1997) to investigate the dynamics of the orientation hypercolumn† constructed in our numerical cortex. This gives us the simulated spatio-temporal response of the hypercolumn to a random sequence of short-duration flashes of oriented grating patterns, which we then analyse in accordance with the method of reverse correlation, as was done in the experiment. Good qualitative agreement with the experiments of Ringach *et al* (1997) is obtained, and comparisons are presented in the conclusions. Preliminary numerical results in this direction were reported by Omurtag *et al* (1999) and by Nykamp and Tranchina (2000). Our investigation thus supports the idea that the feedforward connectivity pattern is insufficient to generate the sharp, contrast-invariant orientation tuning of neurons observed experimentally. The presence or absence of recurrent cortical feedback gives us reverse-correlation responses which match their experimental counterparts for neurons recorded in different cortical layers. Thus, in conjunction with the simulation, the experiment suggests a relationship between cortical layer and connectivity, which the experiment would not have indicated without the simulation.

2. Kinetic equation

To set the stage for the treatment of a hypercolumn of sub-populations, we briefly review the kinetic description of a single population, and follow the notation of the prior publications

† An orientation hypercolumn is a region of cortex that contains neurons tuned to the full range of orientations (0°–180°).

(Knight 2000, Omurtag *et al* 2000, Sirovich *et al* 2000).

In general, the internal state of a neuron is specified by the membrane potential, v, and neuron specific variables that monitor the ionic channels. Since our simulations use the standard integrate-and-fire dynamical model (Tuckwell 1988)

$$\frac{\mathrm{d}v}{\mathrm{d}t} = -\gamma v + s(t); \qquad 0 \leqslant v \leqslant 1 \tag{1}$$

we take the potential v, governed by (1), as a specification of the state of a neuron. Note that the membrane potential has been normalized so that $v = 0$ refers to rest and $v = 1$ to threshold. The coefficient γ, a rate, specifies leakage current, and $s(t)$, also a rate, specifies the synaptic input current. As usual the potential that follows (1) is reset to $v = 0$, on reaching the threshold $v = 1$.

The description of a sub-population begins with the probability density

$$\rho = \rho(v, t) \tag{2}$$

which states the probability $\rho\,\mathrm{d}v$ that we can find a neuron in the population within the membrane potential range $(v, v + \mathrm{d}v)$ at the time t. Then, under general circumstances it can be shown that the time derivative of ρ is equal to minus the divergence of a flux J. In our case this is simply

$$\frac{\partial \rho}{\partial t} = -\frac{\partial J}{\partial v}. \tag{3}$$

For the integrate-and-fire model the flux is given by

$$J(v, t) = -\gamma v \rho + \sigma^{\mathrm{e}} \int_{v-h}^{v} \rho(v', t)\,\mathrm{d}v' - \sigma^{\mathrm{i}} \int_{v}^{v/(1-\kappa)} \rho(v', t)\,\mathrm{d}v'. \tag{4}$$

The first term on the right gives the left-moving flux due to membrane leakage current. In the second term on the right, $\sigma^{\mathrm{e}} = \sigma^{\mathrm{e}}(t)$ denotes the excitatory synaptic arrival rate, and the entire term states that each arrival produces a jump h in the potential ($\sigma^{\mathrm{e}} h$ is thus the corresponding current). Finally, σ^{i} denotes the inhibitory arrival rate, and the term follows the shunting model of inhibition (Tuckwell 1988) for which a voltage-driven, finite synaptic event removes sufficient intracellular electric charge to change the intracellular voltage from $v/(1 - \kappa)$ to v. Partially 'subtractive' inhibition could be incorporated with ease into our model. However this is unlikely to have a significant effect on the firing rates and is not considered. Both h and κ are fairly small compared to unity, and in the simulations described later equation (4) is generalized to accommodate a Gaussian distribution in each of these.

The flux is formally linear in the density ρ, and we emphasize this by writing (3) as

$$\frac{\partial}{\partial t}\rho = Q(\sigma^{\mathrm{e}}, \sigma^{\mathrm{i}})\rho \tag{5}$$

where Q is the linear operator that follows if we substitute (4) into (3). Of particular interest is the firing rate $r(t)$ of the population. Clearly, this is given by the flux of neurons that leave the interval with a jump past threshold at $v = 1$, so that

$$r(t) = J(1, t) = R[\rho(t)]. \tag{6}$$

The last form is meant to indicate that the firing rate is a linear functional of ρ, and the notation is introduced for later convenience. The threshold-reset condition on (1) is taken into account by the periodicity condition on the flux, $J(0, t) = J(1, t)$.

3. The orientation hypercolumn

Our network model is comprised of sub-populations, each of which is described by its own kinetic equation and interactively linked to the others. It consists of interconnected groups of neurons in primary visual cortex that receive input from a small patch of the visual field that projects 0.5 mm^2 on the cortex. We confine our model to orientation tuning, namely, we consider neurons that respond preferentially to edges or bars with a particular orientation. Therefore, the model network is made up of sub-populations that respond preferentially to stimuli presented in each of a range of orientations. The neurons in the model receive direct thalamic input and are interconnected. The populations are parametrized by their orientation preference, $\theta_j = j\pi/N$, $j = 1, \ldots, N$. At each orientation, one excitatory (e) and one inhibitory (i) population is represented. Hence the total number of distinct populations is $2N$. Direction selectivity is not included. Hence the orientation space has a period π. Higher values of N correspond to finer discretization of orientation space. As described above the neurons follow integrate-and-fire dynamics with post-synaptic events, characterized as small jumps in membrane voltage, distributed randomly about a relatively small mean value. We will use the pair of indices, (k, j) to identify the population density $\rho_k(\theta_j)$ of type k (= e or i) and preferred orientation θ_j. The population $\rho_k(\theta_j)$ is stimulated by excitatory and inhibitory impulse rates $\sigma_k^{\mathrm{e}}(\theta_j)$ and $\sigma_k^{\mathrm{i}}(\theta_j)$. Each sub-population is governed by a population equation of the form (5):

$$\frac{\partial \rho_k(\theta_j)}{\partial t} = Q(\sigma_k^{\mathrm{e}}(\theta_j), \sigma_k^{\mathrm{i}}(\theta_j))\rho_k(\theta_j); \qquad k = \mathrm{e}, \mathrm{i}; \qquad j = 1, \ldots, N. \quad (7)$$

To fully specify the equation we need to determine the arrival rates $\sigma_n^m(\theta_j)$, for each choice of m and n, both of which can take the values e, i, for each orientation θ_j. These we take to be

$$\begin{aligned} &\sigma_k^n(\theta_j) = \sum_{m \in P_n} \sum_l c_{km}(|\theta_j - \theta_l|)\, r_n(\theta_l) + \delta_{n\mathrm{e}}\, b_k\, \sigma^o(\theta_j); \\ &n = \mathrm{e}, \mathrm{i}; \qquad j = 1, \ldots, N \end{aligned} \quad (8)$$

an expression whose various features we now discuss in some detail.

P_n is the set of populations that contain neurons of type n. Here $r_n(\theta_l, t) = R[\rho_n(\theta_l, t)]$ is the firing rate of population (n, l), given by (6), and $\sigma^o(\theta_j)$ denotes input from the LGN. The latter is purely excitatory; hence it appears as multiplied by the Kronecker delta ($\delta_{n\mathrm{e}} = 1$ when $n = \mathrm{e}$, $\delta_{n\mathrm{e}} = 0$ otherwise) in the equation. The coupling strength, $c_{km}(|\theta_j - \theta_l|)$, is a function of only the angle difference in orientation space. This expresses the assumption that all orientations are equally represented in the cortex (see Sirovich *et al* 1996 for a general derivation of this form of the assumption and for further discussion of this point).

In order to model the mild orientation selectivity that arrives at the cortex we express the LGN input as a Gaussian profile that is superimposed on a pedestal,

$$\sigma^o(\theta_j) = A_0 + A_1 \mathrm{e}^{[\frac{-(\theta_j - \theta^0)^2}{2\beta^2}]} \equiv W(|\theta_j - \theta^0|), \quad (9)$$

and is broadly tuned ($\beta = \pi/5$ radians $= 36^\circ$). Evidence in support of this form is presented by Somers *et al* (1995), and appears to agree with experimental recordings in the cortex (Ferster *et al* 1996). A_0 and A_1 are fixed parameters that determine the amplitudes of the untuned pedestal and the orientationally tuned profile, respectively. The external input per neuron to the cortex is weighted by the parameter b_k, which indicates the fraction of synapses from the LGN that are made respectively on the inhibitory and excitatory populations. The stimulus orientation is designated by θ^0.

The connectivity between elements in different sub-populations of the hypercolumn is established by a 2×2 matrix that is dependent on the angle difference. A typical component

$c_{km}(|\theta_j - \theta_l|)$ determines the strength of the input from (m, l) to (k, j), where m can be either e or i and similarly for k. The connectivity can be written as a product of two terms

$$c_{km}(|\theta_j - \theta_l|) = T_{km} q_m(|\theta_j - \theta_l|) \tag{10}$$

where T_{km} is determined by the total number of connections between types of neuron in the hypercolumn, regardless of their tuning. Here we follow the modelling of Somers *et al* (1995), which is based on anatomical and electrophysiological data. In particular, we adopt their values of $T_{ee} = 36$, $T_{ei} = 24$, $T_{ie} = 56$, $T_{ii} = 8$.

The distribution of connections in the orientation domain is fixed by $q_m(|\theta_j - \theta_l|)$, which expresses the fraction of connections from (m, l) neurons to neurons tuned to the orientation angle θ_j. The dependence of the distribution on the *donor* type is significant, since excitatory and inhibitory neurons appear to be characterized by different ranges and distributions of synapses. (See, e.g., cross correlation studies by Michalski *et al* (1983) and Hata *et al* (1988), also see references in Somers *et al* (1995); see McLaughlin *et al* (2000) for a different view and model.) We use the general form

$$q_m(|\theta_j - \theta_l|) \propto \begin{cases} \exp\{-(\theta_j - \theta_l)^2/(2\alpha_m^2)\}; & |\theta_j - \theta_l| \leqslant \theta_c \\ 0; & \text{otherwise} \end{cases} \tag{11}$$

where $\theta_c = 60^\circ$ is a cut-off distance, beyond which orientation columns are uncoupled. This conforms to the modelling found in Somers *et al* (1995), where the inhibitory inputs have a broader distribution than the excitatory inputs, $\alpha_i = 60^\circ$ and $\alpha_e = 7.5^\circ$, respectively. Since $q_m(|\theta_j - \theta_l|)$ is defined as the fraction of connections, it follows that $\sum_j q_m(|\theta_j - \theta_l|) = 1$ for all pairs m, l.

The modelling considerations above are sufficient to compute the hypercolumn response to time-independent input as in Somers *et al* (1995). However, computation of response to long sequences of brief stimuli requires modelling of the dynamics of the earlier part of the visual system as well. Temporal input will be confined to signals that arise in M-type retinal ganglion cells, and the relay cells of the LGN will be treated as simple spike-repeaters. (We chose the M-cell response because we are simulating cortical layers with pure M input ($4c\alpha$) and mixed M input (4B).) To implement the ganglion cell response we use the experimentally determined retinal ganglion cell (M-cell) dynamics recently published by Benardete and Kaplan (1999), who include the effects of a retinal contrast gain-control. At 100% contrast and 60 stimuli s^{-1}, according to their measurements, this gain-control would be maximal. In particular they report that for macaque the impulse response increases sharply after the presentation of the stimulus, reaches a peak at approximately 40 ms, then falls to a negative minimum at 60 ms and finally decays exponentially. This measured impulse response integrates to zero over time and is well expressed by

$$E(t) = E_0 \left\{ t^{(N_L - 1)} e^{-\frac{t}{\tau_L}} - \frac{H_s}{\tau_s} \int_0^t ds\, e^{-\frac{t-s}{\tau_s}} s^{(N_L-1)} e^{-\frac{s}{\tau_L}} \right\} \tag{12}$$

where $N_L = 22.71$, $\tau_L = 1.85$ ms, $H_s = 0.97$ ms, $\tau_s = 20$ ms. (Equation (12) is the inverse Fourier transform of the frequency response, determined by measurements, which Benardete and Kaplan (1999) present.) The temporal convolution of this function with the Gaussian distribution $W(|\theta_i - \theta^0|)$ described in (9) yields the time-dependent LGN input to cortex:

$$\sigma^o(\theta_j, t) = \int_0^t W(|\theta_j - \theta^0(s)|) E(t - s)\, ds. \tag{13}$$

Here W is as in equation (9), and $\theta^{(0)}(t)$ repeatedly holds steady for $1/60$ s at values randomly chosen from the set of orientations, as in the experiment of Ringach *et al* (1997). Rather

than the set of 18 orientations used experimentally by Ringach *et al* (1997), we have chosen 32 orientations in order to obtain smoother curves. In all other respects we again use the network and parameters that were advanced by Somers *et al* (1995) as representative, and which were employed in that simulation.

4. Orientation tuning

We first confirm the model's response to time-independent input. Figure 1 (top) shows the anatomically and physiologically based input from the LGN, which we have assumed following Somers *et al* (1995) (right ordinate) and, from solution of the kinetic equations, the corresponding excitatory responses in the cortical hypercolumn (left ordinate, where 'ips' stands for impulses per second). The firing rate per neuron of each orientation column is shown by a solid line connecting successive computed points. Without loss of generality the stimulus orientation has been chosen as $\theta^0 = 0$. These profiles may be interpreted as tuning curves: each shows the variation in response of a typical neuron as stimulus orientation varies from the neuron's preferred orientation. Despite the broadly spread LGN input (dotted curves), the cortical responses are seen to fall rapidly from their maxima, and nearly vanish at approximately 20° away from the preferred orientation. While the amplitude of the response near the preferred orientation increases with contrast, its half-width remains essentially constant. This is in agreement with the contrast invariance of tuning width that was found experimentally by Sclar and Freeman (1982) and by Skottun *et al* (1987). Scrutiny of the data used in plotting figure 1 (top) shows that, as contrast increases, a slight increase in response is elicited at orientations nearly orthogonal to the preferred orientation. This can be attributed to neurons that are tuned to orientations beyond the cut-off distance from the preferred orientation and do not receive inhibitory input from the activity at the preferred orientation. These nearly orthogonal sub-populations, in the model, are therefore the first neural populations tuned to the non-preferred orientations to become active as the contrast increases. Evidence of such behaviour is found in the simulations of Somers *et al* (1995), as well as in experiments (see Sompolinsky and Shapley 1997). The orientation tuning sharpness in figure 1 (top) is robust, within limits, with respect to parameters of the model. A major change, such as reversing the broadness of excitatory and inhibitory connections (by exchanging the values of α_i and α_e) leads to a significant decrease in the sharpness of tuning. If the cortico-cortical coupling is turned off by setting $c_{km}(|\theta_j - \theta_l|) = 0$ for all values of its indices, then the hypercolumn responds with a lower firing rate, and the tuning profile approximately reflects the profile of the input. This is the purely feedforward response that is shown in figure 1 (bottom).

5. Orientation dynamics

In a recent study of Ringach *et al* (1997) the dynamics of orientation tuning was examined experimentally. Cortical cells were stimulated with brief (1/60 s) consecutive presentations of gratings at a set of randomized orientations and four evenly spaced grating phases. The data were analysed by the reverse correlation of nerve impulses with prior presented orientations.

A typical example of the input at the level of cortex is shown in figure 2 (top). We note that its general rate of change with orientation angle is gradual and resembles that of the input in figure 1. The transient peaks along the time axis that are seen in the input become prominent when, by chance, a run of nearby orientations occurs in sequence.

The response of the excitatory neural sub-populations to the input shown in figure 2 (top) is shown in figure 2 (bottom), as calculated by numerical integration of equation (7). We note

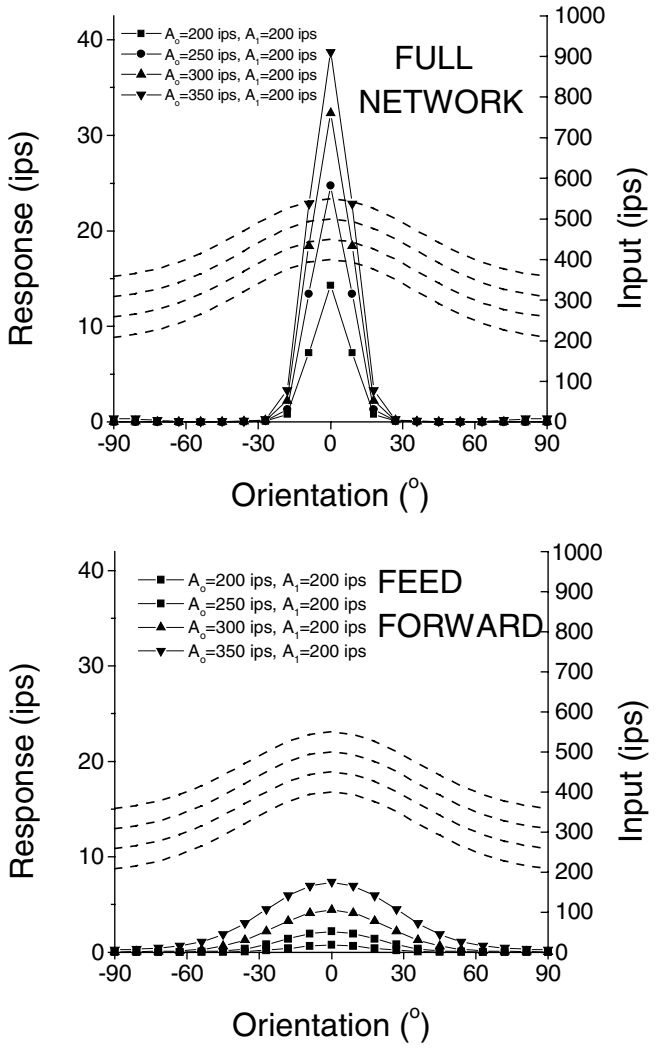

Figure 1. The response (left ordinate) of excitatory cortical neurons receiving steady inputs (right ordinate) from the LGN. Each input is distributed in orientation space (the abscissa) as a broadly tuned Gaussian superimposed on a uniform pedestal. A series of increasingly more intense inputs is shown with the corresponding increasingly larger responses (see (9)). The top panel shows the responses of neurons in the fully connected cortical model. The lower panel shows the responses of neurons for a feedforward network without intra-cortical connections.

that the response has a much sharper orientation profile than does the input, a result that is in agreement with the static case, as seen in figure 1.

6. Reverse correlation methodology

A long-time run of output similar to the sample shown in figure 2 has been analysed in the same way that Ringach *et al* (1997) analysed their experimental data. In the experiment, at the occurrence of a recorded nerve impulse, one goes back τ ms in the orientation time series to record the orientation at that time. This is done for each spike in the experimental record

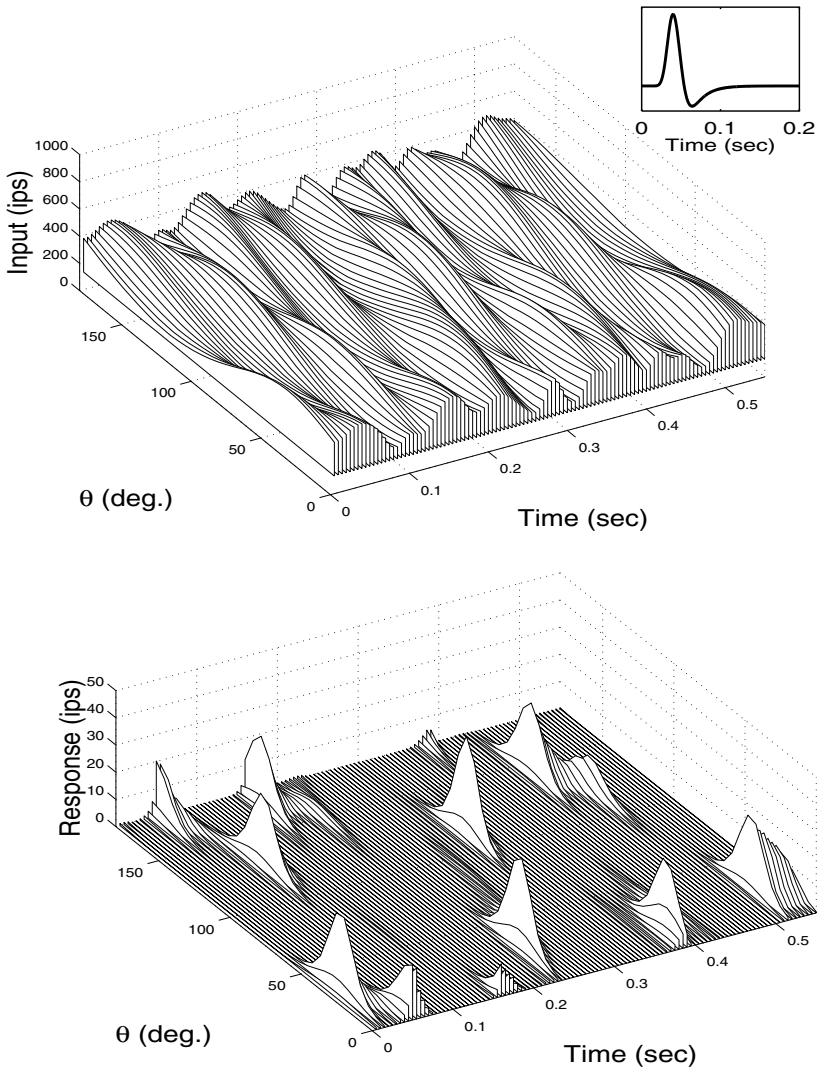

Figure 2. Typical example of time-dependent LGN input to the cortex (top) and the corresponding response of the fully connected cortical network (bottom). The stimuli are briefly (1/60 s) flashed oriented grating patterns. The main figure in the top panel shows that the LGN input varies in a highly complicated way in time and in orientation, while maintaining at any given instant a broad profile in orientation. The inset in the top panel shows the experimentally determined (Benardete and Kaplan 1999) impulse response of M retinal ganglion cells used in modelling the LGN input. The lower panel shows the sharply tuned cortical responses.

and results in an orientation histogram. This process is repeated for all suitable delays τ. The response is the time-sequence of histograms. Our procedure is modified to let us deal with a firing *rate* instead of discrete spikes.

The visual pathway is stimulated with randomly sequenced short duration (1/60 s) oriented patterns. As above we denote the orientation sequence by

$$\theta^0 = \theta^0(t). \tag{14}$$

The short duration of a flash will be denoted by Δt. From the simulation of the hypercolumn

of the populations we obtain the temporal response function

$$r = r(\theta, t) \tag{15}$$

that furnishes the temporal response of the sub-population that has θ for its principal orientation. For the moment θ can be regarded as continuous.

For formal purposes we introduce the characteristic function

$$I(x) = \begin{cases} 1, & x = 0 \\ 0, & x \neq 0. \end{cases} \tag{16}$$

Thus, if $\overline{\theta}$ denotes some fixed orientation then

$$\overline{T} = \int_{-T/2}^{T/2} I(\overline{\theta} - \theta^0(t))\,\mathrm{d}t \tag{17}$$

measures the total time, in the interval $(-T/2, T/2)$, that the oriented stimulus is at $\overline{\theta}$. In the interval $(-T/2, T/2)$ all orientations are equally presented, so $\overline{T}$ is independent of $\overline{\theta}$. The average response to this oriented stimulus at a time τ after $\overline{\theta}$ is presented is then given by

$$P(\theta, \overline{\theta}, \tau) = \frac{1}{\overline{T}} \int_{-T/2}^{T/2} I(\overline{\theta} - \theta^0(t)) r(\theta, t + \tau)\,\mathrm{d}t. \tag{18}$$

Since the duration T is taken to be sufficiently large (formally infinite), we can effect a variable change, which brings (18) to

$$P(\theta, \overline{\theta}, \tau) = \frac{1}{\overline{T}} \int_{-T/2}^{T/2} I(\overline{\theta} - \theta^0(t - \tau)) r(\theta, t)\,\mathrm{d}t. \tag{19}$$

To make contact with the experiment, denote by $\{\bar{t}_j(\tau)\}$ the initial times for which

$$\overline{\theta} - \theta^0(t - \tau) = 0. \tag{20}$$

We may express (19) as

$$P(\theta, \overline{\theta}, \tau) = \frac{1}{\overline{T}} \sum_j \int_{t_j}^{t_j + \Delta t} r(\theta, t_j(\tau) + s)\,\mathrm{d}s \approx \frac{\Delta t}{\overline{T}} \sum_j r(\theta, t_j(\tau)). \tag{21}$$

This yields a histogram for each τ, and incidentally shows that the τ dependent histograms yield the averaged response.

If we denote the angular deviation from $\overline{\theta}$ by

$$\phi = \theta - \overline{\theta} \tag{22}$$

then we can write

$$P = P(\theta, \overline{\theta}, \tau) = f(\phi, \overline{\theta}, \tau). \tag{23}$$

Since all orientations are on an equal footing we can expect the dependence on $\overline{\theta}$ to vanish as $T \uparrow \infty$. Equivalently we can average over $\overline{\theta}$ and we write

$$\overline{f}(\phi, \tau) = \langle f(\phi, \overline{\theta}, \tau) \rangle_{\overline{\theta}}. \tag{24}$$

The average response (24), as a function of orientation disparity and of post-stimulus time, may be directly evaluated from our simulation.

The results below show that, as in Ringach *et al* (1997), the response extracted by reverse correlation has an oriented and sharply peaked early component, followed by a delayed inhibitory component with similar preferred orientation but with broader orientation tuning. This type of response is clearly inconsistent with a simple feedforward architecture, and suggests that cortical processing is involved in the generation of orientation tuning.

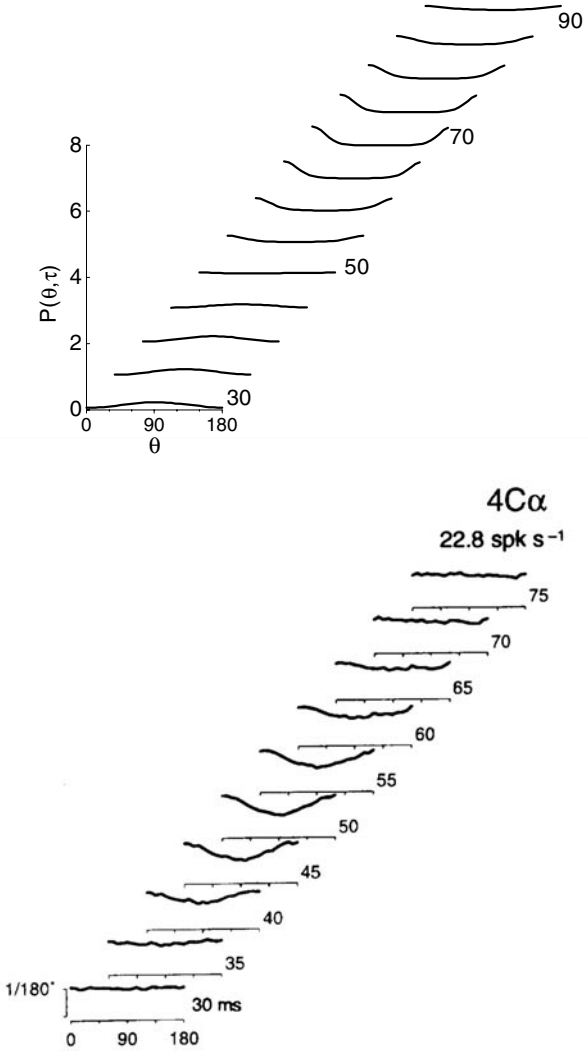

Figure 3. Reverse correlation results for a purely feedforward model (top panel) and for experimentally determined spike trains from layer 4Cα of macaque V1 (lower panel).

7. Reverse correlation results

The measurements of Ringach *et al* (1997) were made in most of the six layers of V1. While it is known that V1 receives input from the LGN in layer 4C and that vertical connections with other layers are present, no unique blueprint for the circuitry has been established. Thus the comparison between the responses of model cells that have different recurrent feedback connectivities and experimentally measured responses of actual cells may be regarded as early evidence concerning what the unknown feedback connectivities of those actual cells might be. In figure 3 we compare our reverse correlation results for a purely feedforward model (lateral connections disabled) with the results of Ringach *et al* (1997) for a cell in layer 4Cα. In both instances there is broad orientation tuning. As in the (Ringach *et al* 1997) experiment, our time

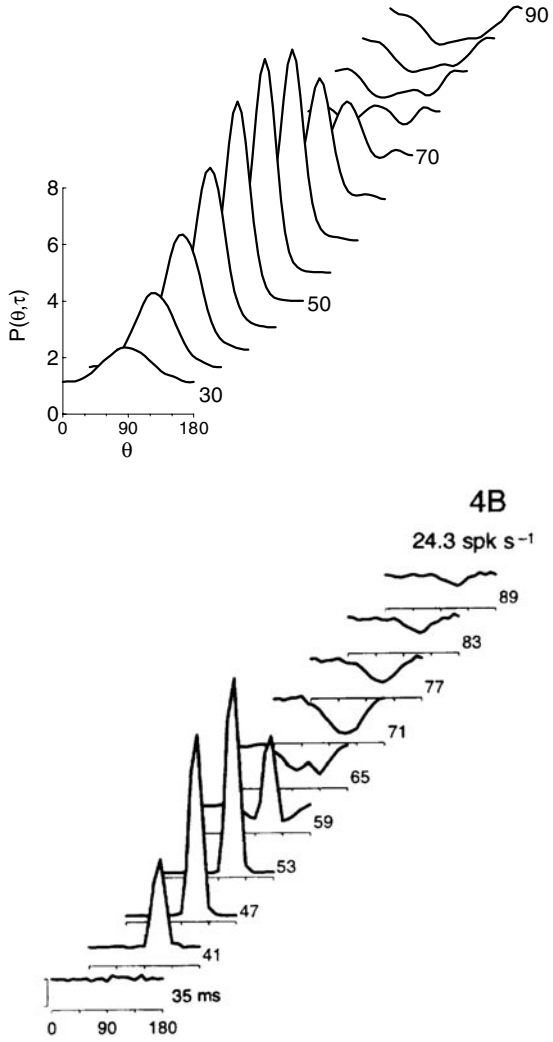

Figure 4. Reverse correlation results for the fully connected cortical network model (top panel) and for experimentally determined spike trains from macaque V1 layer 4B (lower panel).

sequence is nearly monophasic (single rise and fall), even though the M-cell input undergoes both excitatory and inhibitory phases.

In figure 4 we compare the time sequence of orientation traces in the presence of full intracortical connections with the (Ringach *et al* 1997) records for a cell in layer 4B. Again we obtain good qualitative agreement. Our time to maximum is 55 ms compared to 53 ms found in the experiment for layer 4B. It should be observed that inhibitory skirts are a consequence of the simulation, in agreement with the experimental record for layer 4B. Figure 4 shows a passage from peak to trough, another feature common to the simulation and the experimental record. Ringach *et al* (1997) re-normalized the dynamic tuning curve at each τ so that the area under the curve is unity, while we have chosen instead to preserve the equality between

reverse correlation and average response, embodied in (18) and (21). There is little qualitative difference between the two presentations.

Ringach *et al* (1997) point out that many of their recordings exhibit a 'secondary tuning' peak, by which is meant a second peak $\pi/2$ away from the primary peak that occurs at a later time. This same feature appears in our results. In our calculations this feature stems from the fact that the repetitive flashes at random orientations confer a *noise floor* to the system. For the pure feedforward case, shown in figure 3, this is 1.5 ips, while for the interactive case of figure 4 the level is 5.5 ips. For the response exhibited in figure 4, at the maximum time of 55 ms there is a wide inhibitory skirt, so at $\pi/2$ away from the preferred orientation the response vanishes. As remarked for the static tuning curve (figure 1), this is the location that is the first to recover. After the response to the flash at the preferred orientation falls off there is a gradual growth in response to the *noise*, at $\pi/2$ away from the preferred orientation. The time course then follows that dictated by the M-cell impulse response. The result, for the cases shown in figures 3 and 4, are secondary peaks that are local maxima away from and on both sides of the main response at 90°.

8. Discussion

In figure 4 the main features of the experimental reverse-correlation response are replicated by the model response. While systematic discrepancies are visible—the experimental response is somewhat narrower in angle and its rise to peak and return from trough are a little faster—we remember that there has been no fitting of parameters: the cortical parameters are those used by Somers *et al* (1995) to explore the response to time-independent stimuli, while the retinal M-ganglion cell dynamical parameters were taken directly from Benardete and Kaplan (1999). That recurrent cortical feedback is important in forming this response is strongly suggested by the very different dynamical response shown in figure 3, where the cortical feedback was absent. Thus we see that neural simulation of the data-intensive dynamical experiment of Ringach *et al* (1997) contributes further evidence that cortical feedback is important in the response of a cortical orientation hypercolumn.

Our simulation of cortical dynamics in a data-intensive experiment was made feasible by employing the population kinetics equations, which represent the dynamics of a large collection of neurons in a manner that is far more efficient than is the use of many individual neuron replicas in a direct simulation. Depending on details of the approach, several orders of magnitude in computational speed are easily realizable in this way.

For time-independent calculations such as that of Somers *et al* (1995), an efficient alternative for obtaining approximate features is the use of mean-field theory as advanced by Wilson and Cowan (1973), which postulates a simplified dynamics for the firing rate itself. In the context of an orientation hypercolumn this has been carried out by Ben-Yishai *et al* (1995), with results comparable to those of Somers *et al* (1995) and to the time-independent results shown in figure 1. However, several central features of neuron population dynamics, which are brought to the foreground by the population kinetics equations, are absent from such firing rate or mean-field approaches. The mean-field approach has difficulty following stimuli that are changing rapidly (Gerstner 1995 and references therein). Population equations as developed here respond immediately to inputs and follow the rapid dynamics neglected in the mean-field approximation. Three recent studies (Gerstner 2000, Knight *et al* 2000, Nykamp and Tranchina 2000), in which a step transient response is investigated, all show a hunting oscillatory response which is absent from a mean-field theory.

A population kinetics, in the diffusion limit, applied to visual cortex, that appears to share some features with our presentation, is reported in the recent brief note of Adorjan *et al* (1999).

(See Omurtag *et al* 2000 for limitations of the diffusion approximation.) Similar population kinetics is applied to the time-independent stimulus case of Somers *et al* (1995) by Nykamp and Tranchina (2000).

9. Concluding remarks

We have shown that the use of the kinetic equation enables a cortical simulation of a data-intensive dynamical experiment. Our simulation supports the notion that cortical processing plays an important role in the orientation selectivity of visual cortex. The functional significance of cortical connections is strongly supported by anatomical estimates of the relative size of cortical input compared to thalamic input in layer 4 (e.g. Peters *et al* 1994). Modelling of the same phenomena by direct simulation would have presented a prohibitive computational effort, whereas our present approach leads to a modest calculation†. The technique is a general one, and its computational advantage can be used to address other large-scale cortical simulations.

Acknowledgments

This work has been supported by NIH/NEI EY11276, NIH/NIMH MH50166, NIH/NEI EY01867 and ONR N00014-96-1-0492. Ehud Kaplan is the Jules and Doris Stein Research to Prevent Blindness Professor at the Ophthalmology Department at Mt Sinai.

References

Adorjan P, Barna G, Erdi P and Obermayer K 1999 A statistical neural field approach to orientation selectivity *Neurocomputing* **26** 477–82

Adorjan P, Levitt J, Lund J and Obermayer K 1999 A model for the intracortical origin of orientation preference and tuning in macaque striate cortex *Visual Neurosci.* **12** 303–18

Ben-Yishai R, Bar-Or R L and Sompolinsky H 1995 Theory of orientation tuning in visual cortex *Proc. Natl Acad. Sci. USA* **92** 3844–8

Benardete E and Kaplan E 1999 The dynamics of primate M retinal ganglion cells *Visual Neurosci.* **16** 355–68

Blasdel G 1992 Differential imaging of ocular dominance and orientation selectivity in monkey striate cortex *J. Neurosci.* **12** 3115–38

Bonhoeffer T and Grinvald A 1991 Iso-orientation domains in cat visual cortex are arranged in pinwheel-like patterns *Nature* **353** 267–94

Das A 1996 Orientation in visual cortex: a simple mechanism emerges *Neuron* **16** 447–80

de Boer E and Kuyper P 1968 Triggered correlation *IEEE Trans. Biomed. Eng.* **15** 281–4

Ferster D, Chuing S and Wheat H 1996 Orientation selectivity of thalamic input to simple cells of cat visual cortex *Nature* **380** 249–52

Gerstner W 1995 Time structure of the activity in neural network models *Phys. Rev.* E **51** 738–58

——2000 Population dynamics of spiking neurons: fast transients, asynchronous states and locking *Neural Comput.* **12** 43–89

Hata Y, Tsumoto T, Sato H, Hagihara K and Tamura H 1988 Inhibition contributes to orientation selectivity in visual cortex of cat *Nature* **335** 815–7

Hubel D and Wiesel T 1962 Receptive fields, binocular interaction and functional architecture in the cat's visual cortex *J. Physiol. Lond.* **160** 106–54

——1968 Receptive fields and functional architecture of monkey striate cortex *J. Physiol. Lond.* **195** 215–45

——1974 Sequence regularity and geometry of orientation columns in the monkey striate cortex *J. Comp. Neurol.* **158** 267–94

† For a population of 90 000 integrate-and-fire neurons, a saving in computational time of two orders of magnitude is obtained. This saving can be further increased by low-dimensional approximations of the kinetic equation (Knight 2000).

Jones J and Palmer L 1987 The two-dimensional spatial structure of simple receptive fields in cat striate cortex *J. Neurophysiol.* **58** 1187–211

Knight B 2000 Dynamics of encoding in neuron populations: some general mathematical features *Neural Comput.* **12** 473–518

Knight B, Manin D and Sirovich L 1996 Dynamical models of interacting neuron populations *Symp. on Robotics and Cybernetics: Computational Engineering in Systems Applications* ed E C Gerf (Lille: Cite Scientifique)

Knight B, Omurtag A and Sirovich L 2000 The approach of a neuron population firing rate to a new equilibrium: an exact theoretical result *Neural Comput.* **12** 1045–55

McLaughlin D, Shapley R, Shelley M and Wielaard D 2000 A neural network model of macaque primary visual cortex (v1): orientation selectivity and dynamics in the input layer 4cα *Proc. Natl Acad. Sci. USA* **97** 8087–92

Michalski A, Gerstein G, Czarkowska J and Tarnecki R 1983 Interactions between cat striate cortex neurons *Exp. Brain Res.* **51** 97–107

Nykamp D and Tranchina D 2000 A population density approach that facilitates large-scale modelling of neural networks: analysis and an application to orientation tuning *J. Comp. Neurosci.* **8** 19–50

Omurtag A, Knight B, Kaplan E and Sirovich L 1999 Efficient simulation of large neuronal populations: an investigation of orientation tuning in the visual cortex *Invest. Ophthalmol. Visual Sci.* **40** S3018

Omurtag A, Knight B and Sirovich L 2000 On the simulation of large populations of neurons *J. Comp. Neurosci.* **8** 51–63

Peters A, Payne B and Budd J 1994 A numerical analysis of the geniculocortical input to striate cortex in the monkey *Cerebral Cortex* **4** 215–29

Ringach D, Hawken M and Shapley R 1997 Dynamics of orientation tuning in macaque primary visual cortex *Nature* **387** 281–4

Sclar G and Freeman R 1982 Orientation selectivity in cat's striate cortex is invariant with stimulus contrast *Exp. Brain Res.* **46** 457–61

Sirovich L, Everson R, Kaplan E, Knight B, O'Brien E and Orbach D 1996 Modeling the functional organization of the visual cortex *Physica* D **96** 355–66

Sirovich L, Knight B and Omurtag A 2000 Dynamics of neuronal populations: the equilibrium solution *SIAM J. Appl. Math.* **60** 2009–28

Skottun B, Bradley A, Sclar G, Ohzawa I and Freeman R 1987 The effect of contrast on visual orientation and spatial frequency discrimination: a comparison of single cells and behavior *J. Neurophysiol.* **57** 773–86

Somers D, Nelson S and Sur M 1995 An emergent model of orientation selectivity in cat visual cortex simple cells *J. Neurosci.* **15** 5448–65

Sompolinsky H and Shapley R 1997 New perspectives on the mechanisms for orientation selectivity *Curr. Opin. Neurobiol.* **7** 514–22

Tuckwell H 1988 *Introduction to Theoretical Neurobiology* vol 2 (Cambridge: Cambridge University Press) ch 9

Wilson H and Cowan J 1973 A mathematical theory of the functional dynamics of cortical and thalamic nervous tissue *Kybernetik* **13** 55–80